



OPEN

Thioflavin-positive tau aggregates complicating quantification of amyloid plaques in the brain of 5XFAD transgenic mouse model

Jisu Shin, Sohui Park, HeeYang Lee & YoungSoo Kim

Transgenic mouse models recapitulating Alzheimer's disease (AD) pathology are pivotal in molecular studies and drug evaluation. In transgenic models selectively expressing amyloid- β (A β), thioflavin S (ThS), a fluorescent dye with β -sheet binding properties, is widely employed to observe amyloid plaque accumulation. In this study, we investigated the possibility that a commonly used A β -expressing AD model mouse, 5XFAD, generates ThS-positive aggregates of β -sheet structures in addition to A β fibrils. To test this hypothesis, brain sections of male and female 5XFAD mice were double-stained with ThS and monoclonal antibodies against A β , tau, or α -synuclein, all of which aggregates are detected by ThS. Our results revealed that, in addition to amyloid plaques, 5XFAD mice express ThS-positive phospho-tau (p-tau) aggregates. Upon administration of a small molecule that exclusively disaggregates A β to 5XFAD mice for six weeks, we found that the reduction level of plaques was smaller in brain sections stained by ThS compared to an anti-A β antibody. Our findings implicate that the use of ThS complicates the quantification of amyloid plaques and the assessment of A β -targeting drugs in 5XFAD mice.

Alzheimer's disease (AD) is defined by accumulation of amyloid- β (A β) plaques and neurofibrillary tau tangles in the brain, leading to neurodegeneration and cognitive dysfunction¹. The need for deeper molecular understanding underlying AD pathogenesis and the discovery of effective therapeutics has led to the development of transgenic mouse models mimicking A β and tau pathologies. These neuropathological alterations in the brain are directly visualized by dyes, providing valuable information as an indicator of disease progression. As plaques and tangles share a common β -sheet-rich structure, both on the brain tissue are stained by β -sheet-binding dyes such as thioflavin S (ThS)^{2,3}. Besides these AD-related proteins, ThS also binds to other β -sheet-containing deposits such as Lewy bodies of α -synuclein^{4,5}.

5XFAD is a well-validated and widely used transgenic mouse model of AD that possesses a total of five mutations in amyloid precursor protein (APP) and presenilin (PSEN1) genes, which are involved in A β production. Swedish (K670N/M671L), Florida (I716V), and London (V717I) mutations in APP genes, and M146L and L286V mutations in PSEN1 genes contribute to the rapid development of A β deposits and progressive cognitive decline in 5XFAD mice. As the 5XFAD mouse model was originally generated to only develop amyloid pathology, single-staining with ThS is widely used for A β plaque detection^{6–11}.

In A β -expressing transgenic mouse models such as 5XFAD, the therapeutic effects of A β -targeting drugs can be evaluated through the changes in the amount of ThS-stained aggregates. However, while evaluating the efficacy of A β -targeting drugs in ThS-stained brains of 5XFAD mice, we found that drugs that were previously shown to effectively reduce plaques in APP/PS1 double transgenic mice had less effect in 5XFAD mice. Therefore, we hypothesized that 5XFAD mice express β -sheet-rich proteins other than A β , which may have ostensibly caused such results in ThS-stained mice brains. To identify the protein component of ThS-positive aggregates, male 5XFAD mice from 7 to 8 months of age and female from 5 to 6 months of age were prepared. Their brain sections were double-stained by ThS with anti-A β (1–16) monoclonal antibody 6E10, anti-A β (17–24) monoclonal antibody 4G8, anti-phosphorylated tau monoclonal antibody AT8, or anti- α -synuclein monoclonal antibody (Table 1). For further validation of our hypothesis that the non-specific detection of ThS against multiple protein aggregates may complicate A β quantification and A β -targeting drug evaluation in 5XFAD mice, an A β -dissociating chemical EPPS at a concentration of 100 mg/kg was orally administered to 6-month-old male mice in drinking water for six weeks (Table 1)¹². Subsequently, the brains of vehicle- or EPPS-treated mice were

Department of Pharmacy, Yonsei University, Incheon 21983, Republic of Korea. email: y.kim@yonsei.ac.kr

Age (months)	Gender	Number of mice	Markers	Brain regions
7–8	Male	3	ThS/6E10	Whole Cortex Hippocampus
			ThS/AT8	
			ThS/ α -Synuclein	
5–6	Female	3	ThS/6E10	Whole Cortex Hippocampus
			ThS/AT8	
			ThS/ α -Synuclein	
5–6	Female	3	ThS/4G8	Whole Cortex Hippocampus
7.5 (including 6 weeks of drug administration)	Male	5 (Vehicle)	ThS/6E10	Whole Cortex Hippocampus
		4 (EPPS)	ThS/AT8	

Table 1. Mice preparation for histochemical analyses and drug administration.

double-stained by ThS with either 6E10 or AT8 to compare the differences between the number of ThS-positive aggregates and each antibody stained accumulates.

Results

ThS-positive and AT8-positive phospho-tau aggregates found in 5XFAD mouse brain. To compare the type and the quantity of protein aggregates stained by ThS and aforementioned antibodies in the brain of 5XFAD, male ($n=3$) and female ($n=3$) 5XFAD mice were sacrificed at 7–8 months and 5–6 months of age, respectively. As female mice develop cerebral A β burden faster than males⁸, we used females one month younger than males in this study. For A β plaque detection, mouse brain sections were double-stained with ThS and 6E10, which is reactive to residue 1–16 of A β (Fig. 1a). In 5XFAD mouse brain, β -sheet-rich protein aggregates detected by ThS were thought to be A β plaques, which can be also stained by 6E10. However, besides the co-stained A β plaques (white circles in Fig. 1b), there was a significant number of 6E10-negative aggregates that were positive for ThS, in cortical and hippocampal regions of both male and female brains (white arrows in Fig. 1b). In both male and female mouse brains, the number of 6E10-negative aggregates, which appeared as green dots by only ThS fluorescent signal, was more than that of A β plaques shown as yellow dots by merged fluorescence (Fig. 1b). This observation seems improbable because 6E10 detect not only dense core plaques but also diffuse plaques, while ThS can only label dense core plaques in the brain of APP/PSEN1-expressing mouse models^{13,14}. In addition, we confirmed the possibility that truncated A β species appears to be non-A β , represented as green fluorescent signals, because 6E10 binds to N-terminus of A β . The brain of female 5XFAD mice ($n=3$) at 5–6 months of age were double-stained with ThS and 4G8, which is reactive to residue 17–24 of A β (Fig. 1c–e). As a similar result of 6E10 staining, along with the numerous A β plaques double-stained by ThS and 4G8 (white circles in Fig. 1e), 4G8-negative aggregates were also observed (white arrows in Fig. 1e) in both cortical and hippocampal regions.

To identify the components of ThS-positive protein aggregates that were not stained by 6E10 and 4G8, brain sections were double-stained with ThS and AT8 (Fig. 2a) or α -synuclein antibody (Fig. 3a). AT8 staining revealed aggregated tau composed of phosphorylated tau at both Ser202 and Thr205 in brains of both genders, and the labeled structures overlapped with ThS (white circles in Fig. 2b). In brains stained with α -synuclein antibody, which recognizes amino acids 15–123 of α -synuclein, both genders of 5XFAD mice and wild type mice did not display detectable signals (Fig. 3a,b).

To confirm that yellow fluorescent signals in merged images were not due to the spectral overlap of ThS, we performed single-labeling with AT8 (Fig. 2c) or α -synuclein antibody (Fig. 3c). While AT8 single-staining showed a significant amount of tau aggregates in male and female 5XFAD mouse brains compared to age- and gender-matched wild type mouse brains, single-staining with α -synuclein antibody did not demonstrate visible fluorescence of α -synuclein. Therefore, we concluded that both male and female 5XFAD mice express aggregated phospho-tau (p-tau) that were detected by ThS.

Complicated interpretation of A β -targeting drug upon ThS brain staining. To show the discrepancies between ThS and 6E10 staining in A β detection, 6-month-old male 5XFAD mice were administered 100 mg/kg of EPPS, a previously reported A β -plaque-dissociating molecule^{12,15}, via drinking water for six weeks. After the administration, the disaggregating effect of EPPS on A β plaques in the brain was evaluated by histochemistry using ThS with 6E10 or AT8 (Fig. 4a–c). Congruous with the previous study^{12,15}, a greater reduction in the number of A β plaques was observed in brains stained with 6E10 (Fig. 4b); 46% (total area), 49% (hippocampus), and 68% (cortex) of 6E10-stained plaques remained after EPPS treatment when plaque numbers of the vehicle group were normalized to 100%. However, ThS staining diminished the difference of aggregate amount between the two groups; 80% (total area), 74% (hippocampus), and 90% (cortex) of aggregates in the brain of EPPS-administered mice compared to vehicle-administered mice. The average percentages of plaque reduction by EPPS administration in 6E10 and ThS staining were 45.7% and 18.7%, respectively (Supplementary Fig. S1). Collectively, we deduced that this discrepancy between two staining methods may be attributed to that ThS-positive p-tau aggregates complicate the quantification of plaques in the brains of 5XFAD mice, leading to incorrect validation of drug efficacy (Fig. 4a–c). In conclusion, cross-checking data with an A β -specific antibody is recommended in the evaluation of A β -targeting drugs.

Discussion

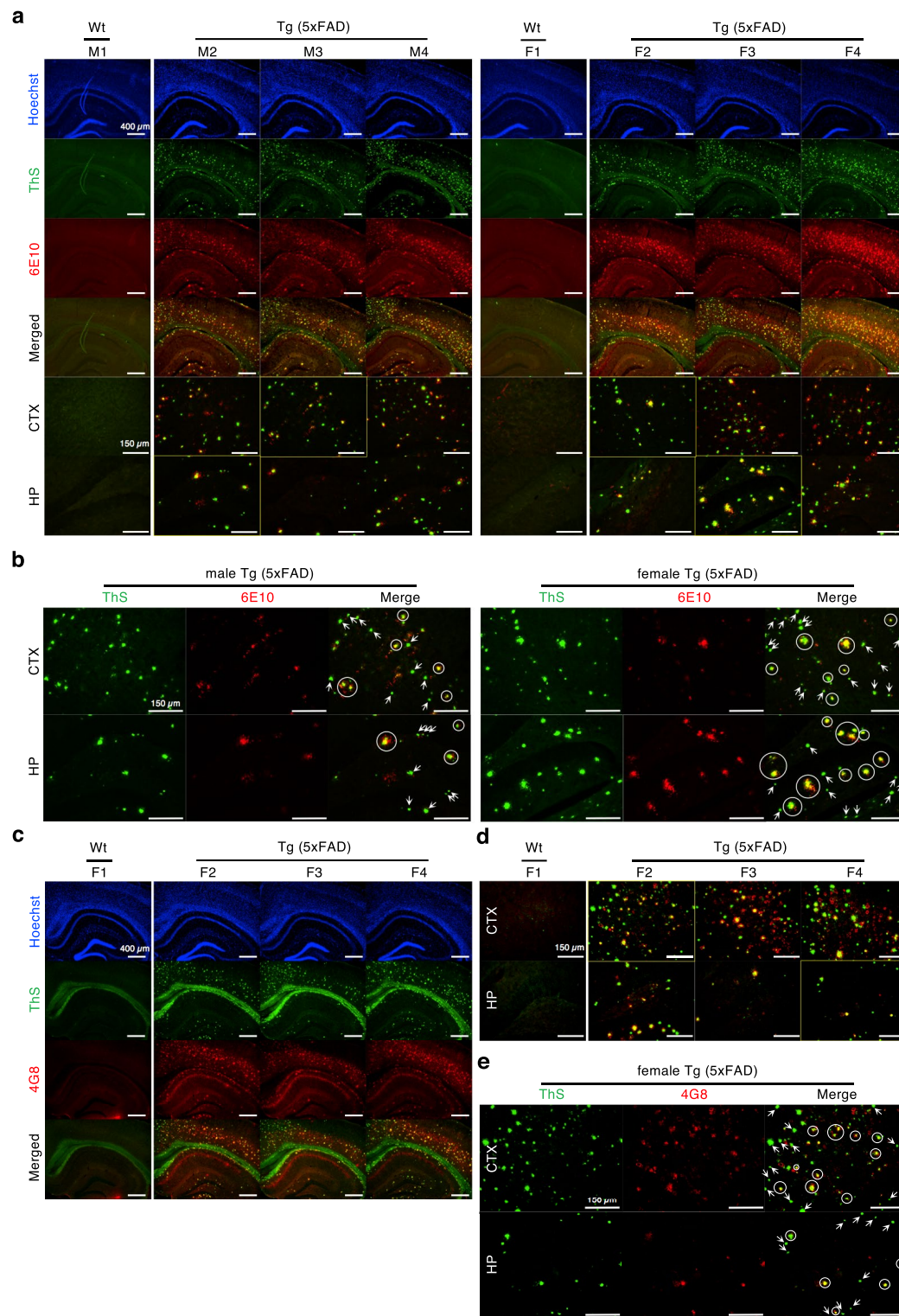
Here, we report that single-staining with ThS for A β plaque measurements in the 5XFAD mouse brains can lead to incorrect interpretation because 5XFAD exhibits ThS-positive p-tau aggregates in their brains. We observed ThS-labeled insoluble protein aggregates that were not positive for anti-A β antibodies, 6E10 or 4G8, in the cortical and hippocampal regions of both male and female 5XFAD mice. Considering the possibility that the ThS + /anti-A β aggregates— could be composed of other aggregation-prone proteins, the brain sections of 5XFAD mice were stained with antibodies against phosphorylated tau and α -synuclein. Through double-staining with ThS and AT8, we deduced that the ThS + /anti-A β aggregates—were p-tau aggregates, ThS + /anti-hyperphosphorylated tau +. To test whether A β quantification with ThS in 5XFAD mouse brains interferes the evaluation of the efficacy of anti-A β drug, 5XFAD mice were orally administered an A β -dissociating agent, EPPS, and their brains were double-stained by ThS with 6E10 or AT8. We found that ThS-stained brains displayed a smaller extent of EPPS-induced plaque reduction than in the same brains stained with 6E10, demonstrating the need for extra attention in the use of ThS as an A β -detecting probe in 5XFAD mice.

As the 5XFAD mouse model was originally designed for the investigation of APP- and A β -related pathology, this model is not expected to develop significant tauopathy in the brain. Subsequently, tau aggregates were reported to be absent in this model when using a phosphorylated tau antibody recognizing phosphorylation at Ser199/202^{8,16}. However, recent studies revealed that 5XFAD mice display a gradual increase of total tau level in cerebrospinal fluid¹⁷ as well as significant aggregated p-tau stained by AT8 recognizing phosphorylation at Ser202 and Thr205^{18,19}. Furthermore, accumulating reports indicate that a pretangle state, in which tau is phosphorylated and accumulated²⁰, was observed in A β -overexpressing transgenic mouse models including 5XFAD mice^{21–25}. Consistent with these results, we observed ThS-positive tau phenotypes in the brains of both male and female aged 5XFAD mice by double-staining with ThS and AT8. As the tau hyperphosphorylation plays a critical role as a trigger for the development of neurofibrillary tangles, further investigation is needed to demonstrate the exact mechanisms on the alterations of endogenous tau in pretangle state of A β -overexpressing mouse models. The further analyses are also required to investigate the phosphorylation of the other pathologic tau epitopes in the brain of 5XFAD mice, except for Ser202 and Thr205 that were detected by AT8 antibody. Additionally, an in-depth study on whether these p-tau aggregates were neurofibrillary tau tangles or phospho-tau within dystrophic neurites surrounding A β plaques is also warranted.

To conclude, due to the presence of p-tau aggregates in the brain of 5XFAD mice, the use of ThS in A β quantification in this model requires caution since binding property of ThS against both A β and tau aggregates can lead inaccurate results. As these findings were only observed in the specific age of mice, further studies are needed to confirm age-dependent accumulation of tau in the brain of both male and female 5XFAD mice. Furthermore, the presence of phosphorylated tau at other epitopes also needs to be investigated.

Materials and methods

Animals. For histochemical analysis, male 5XFAD mice (strain name; B6SJL-Tg(APPswF1L_{on},PSEN1*^{M14}6L*L286V)6799Vas/Mmjax) from 7 to 8 months of age (n = 3) and female from 5 to 6 months of age (n = 6) were obtained from Jackson Laboratory (USA). Age- and gender-matched wild type mice (n = 1, each) were used as



◀ **Figure 1.** ThS stains A β plaques in 5XFAD mice brains and other protein aggregates as well. **(a)** The brains were double-stained by ThS and 6E10 anti-A β antibody. 7–8-month-old male (M2–M4) and 5–6-month-old female (F2–F4) 5XFAD mice were used. The brain of age-matched B6SJL wild type male (M1) or female mouse (F1) was also stained as a control. Hoechst 33342 was applied for nuclear counterstaining (scale bars = 400 μ m, 150 μ m). **(b)** The representative image of ThS- or 6E10-stained brains, which is indicated as yellow boxed images in **(a)** (scale bars = 150 μ m). In merged images, yellow dots in white circles represent the double-staining of ThS and 6E10, whereas green dots marked by white arrows indicated 6E10-negative, ThS-positive aggregates. **(c)** ThS and 4G8 double-stained female 5XFAD brains at age of 5–6-month-old (F2–F4). The brain of age-matched B6SJL wild type female mouse (F1) was also stained as a control. Hoechst 33342 was used for nuclear counterstaining (scale bars = 400 μ m). **(d)** Merged images of ThS and 4G8 double-staining (scale bars = 150 μ m). **(e)** The representative image of ThS- or 4G8-stained brains, which is indicated as yellow boxed images in **(d)**. In merged images of cortical and hippocampal regions, yellow dots in white circles indicated the double-staining of ThS and 4G8, while green dots marked by white arrows represented 4G8-negative, ThS-positive aggregates (scale bars = 150 μ m). wt, wild type; Tg, transgenic; ThS, thioflavin S; CTX, cortex; HP, hippocampus.

controls. All mice were bred and provided constant temperature, humidity, and 12:12 h light–dark cycle in the animal facility of Yonsei University. Mice were given ad libitum access to water and food. All animal experiments were carried out in accordance with the National Institutes of Health guide for the care and use of laboratory animals (NIH Publications) as well as the ARRIVE guidelines and approved by the Animal Institutional Animal Care and Use Committee of Yonsei University (Korea, IACUC-202003–1038-01).

Drug administration. A dose of 100 mg/kg of EPPS (Sigma-Aldrich, USA), a previously reported A β -dissociating drug candidate, was freely administered to 6-month-old male 5XFAD mice ($n = 4$) via drinking water for six weeks. After the administration, all mice were deeply anesthetized by intraperitoneal injection of 4% avertin (2,2,2-Tribromoethanol, Sigma-Aldrich, USA) and sacrificed by cervical dislocation to obtain brain tissue samples and compare the number of labeled plaques by 6E10 antibody and ThS. Age- and gender-matched 5XFAD transgenic mice ($n = 5$) and B6/SJL wild type mice ($n = 4$) were also sacrificed as controls.

Histochemistry. All mice were deeply anesthetized by intraperitoneal injection of 4% avertin for the brain extraction. After perfusion with 0.9% NaCl, mice were sacrificed by cervical dislocation and extracted brains were fixed in 4% paraformaldehyde (Biosesang, Korea). After 24 h of fixation, brains were immersed in 30% sucrose for 2 days. For immunofluorescence staining, 35 μ m-thick frozen sections were incubated with 6E10 (Biolegend, USA, Catalog# SIG-39320, 1:200), 4G8 (Biolegend, USA, Catalog# SIG-39220, 1:200), AT8 (Invitrogen, USA, Catalog# MN1020, 1:200), or α -synuclein (BD Transduction Laboratories, USA, Catalog# 610786, 1:250) antibody diluted in 5% horse serum (Gibco, USA), then with Alexa555-conjugated secondary antibody (1:200 in PBS). Each stained section was incubated in 500 μ M of Thioflavin S (ThS, Sigma-Aldrich, USA) dissolved in 50% ethanol for 7 min for ThS double-staining. Hoechst 33342 (10 μ g/mL, Sigma-Aldrich, USA) was used to observe nuclear morphology. All images were taken using a fluorescence microscope (Leica DM2500, Germany). The number and area of plaques detected by ThS and 6E10 were quantified using Image J software.

Statistical analysis. Graphs were obtained by GraphPad Prism 7 and statistical analyses were performed using unpaired two-tailed Student's *t*-test. All data were represented as mean \pm SEM.

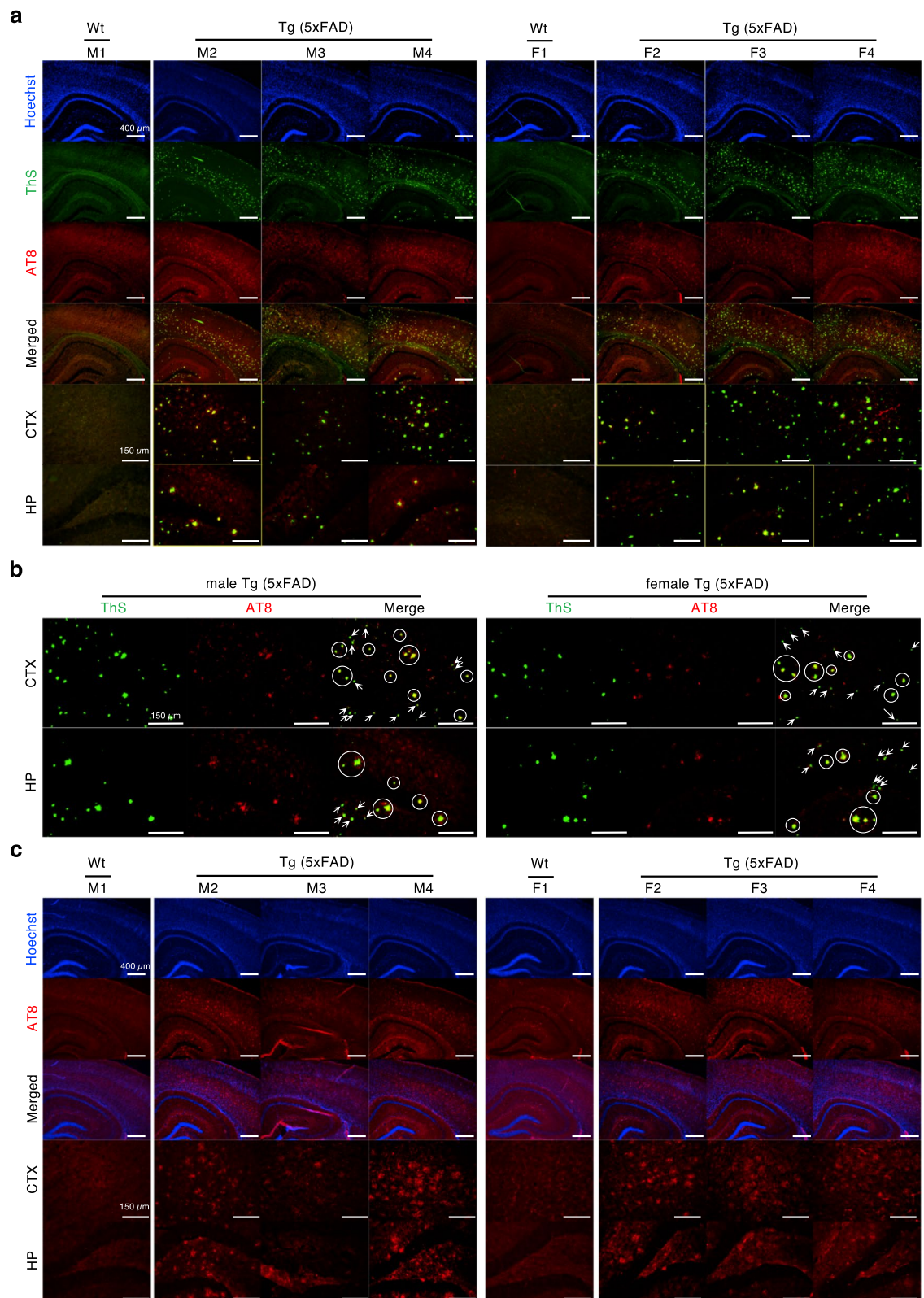


Figure 2. P-tau aggregates in 5XFAD mice brains were stained by AT8 antibody and ThS. (a) The brains were double-stained by Thioflavin S and AT8 anti-phosphorylated tau antibody. We used male (M2-M4) and female (F2-F4) 5XFAD mice at 7–8 months and 5–6 months of age, respectively. The brain of age- and gender-matched B6SJL wild type male (M1 and F1) was also stained as a control. Hoechst 33342 was used for visualization of nuclei (Scale bars = 400 μ m, 150 μ m). (b) The representative image of ThS- or AT8-stained brains, which is indicated as yellow boxed images in (a) (scale bars = 150 μ m). Yellow dots of overlapped fluorescence in white circles represent the aggregated p-tau double-stained by ThS and AT8, whereas green dots marked by white arrows indicate ThS-positive aggregates that were not p-tau aggregates. (c) Single-labeling with AT8 antibody showed 5XFAD mouse brains exhibit significant amount of aggregated p-tau compared to wild type mouse brains (Scale bars = 400 μ m, 150 μ m). wt, wild type; Tg, transgenic; ThS, thioflavin S; CTX, cortex; HP, hippocampus.

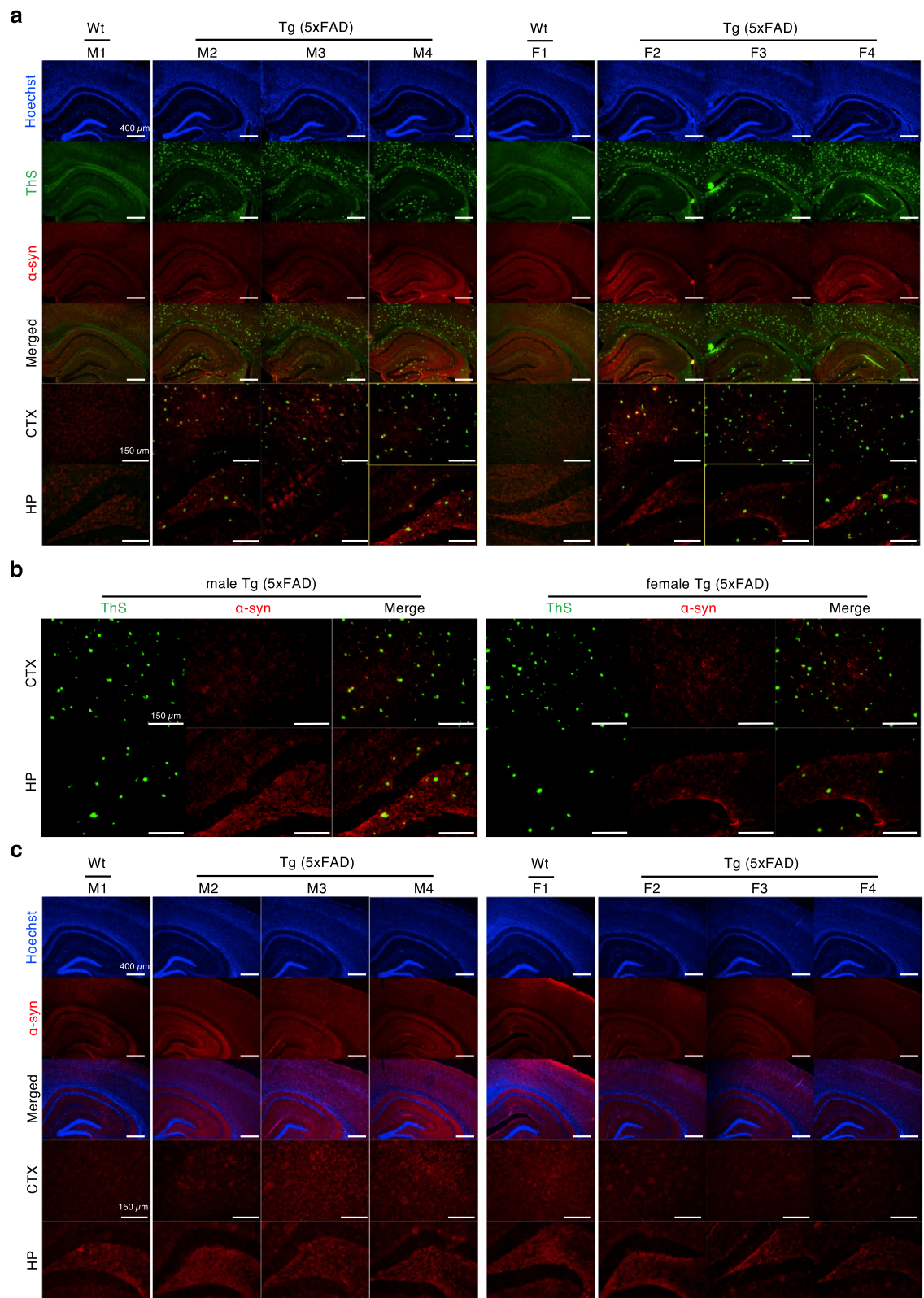


Figure 3. α -Synuclein aggregates were not detected in 5XFAD mice brains. **(a)** The brains were double-stained by Thioflavin S and AT8 anti- α -synuclein antibody. We used male (M2–M4) and female (F2–F4) 5XFAD mice at 7–8 months and 5–6 months of age, respectively. Age- and gender-matched B6SJL wild type male (M1 and F1) was used for a control (scale bars = 400 μ m, 150 μ m). **(b)** The representative image of ThS- or α -synuclein-stained brains, which is indicated as yellow boxed images in **(a)**. Several green dots of ThS fluorescence were observed but no overlapped signal was detected in double-staining by ThS and α -synuclein (scale bars = 150 μ m). **(c)** Single-labeling α -synuclein with α -synuclein antibody displayed no remarkable α -synuclein aggregates in 5XFAD mouse brains compared to wild type mouse brains (scale bars = 400 μ m, 150 μ m). wt, wild type; Tg, transgenic; ThS, thioflavin S; α -syn, α -synuclein; CTX, cortex; HP, hippocampus.

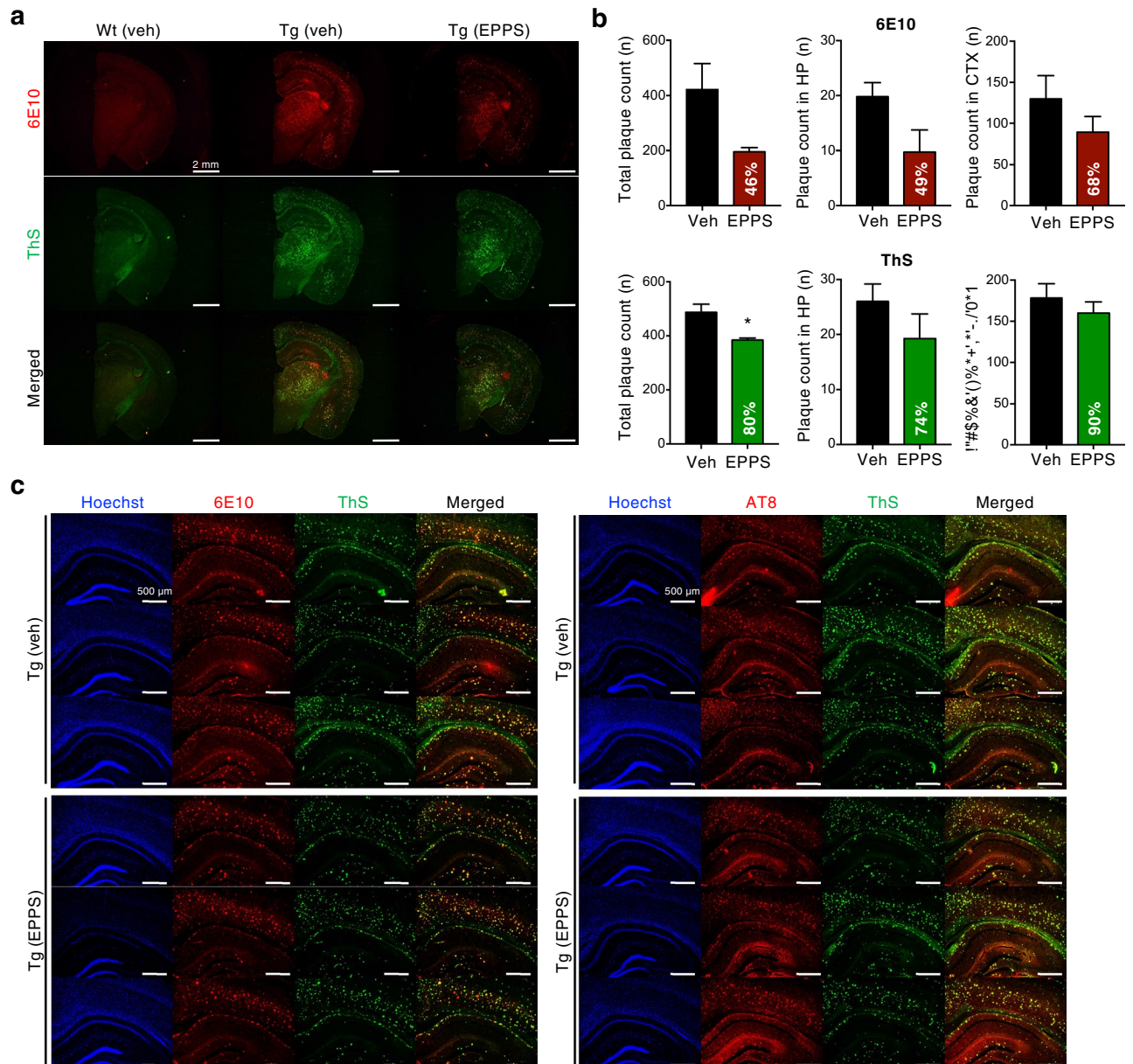


Figure 4. The different number of plaques were detected in 6E10- and ThS-stained 5XFAD mouse brains after the treatment of Aβ-disaggregating drug, EPPS. (a) The representative 6E10- and ThS-stained fluorescence half-brain images of the vehicle-treated wild type mouse, and vehicle- and EPPS-treated 5XFAD mice (scale bars = 2 mm). (b) Quantification of Aβ plaques in whole, hippocampal, and cortical regions of 6E10- or ThS-stained half-brains. The amount of remaining aggregates of EPPS group shown as a percentage in the bar graphs were normalized to the plaque numbers of vehicle group (100%). Significance was tested by unpaired two-tailed student's *t*-test (**P* < 0.05, other comparisons were not significant). (c) Individual and merged brain images of the vehicle- and EPPS administered- groups stained with ThS and 6E10 or AT8 antibody (scale bars = 500 μm). wt, wild type; Tg, transgenic; veh, vehicle; ThS, thioflavin S; CTX, cortex; HP, hippocampus.

Received: 5 November 2020; Accepted: 6 January 2021
Published online: 15 January 2021

References

- Kametani, F. & Hasegawa, M. Reconsideration of amyloid hypothesis and tau hypothesis in Alzheimer's disease. *Front. Neurosci.* **12**, 25–35 (2018).
- DeVos, S. L. *et al.* Tau reduction in the presence of amyloid-beta prevents tau pathology and neuronal death in vivo. *Brain* **141**, 2194–2212 (2018).
- Glenner, G. G. Amyloid deposits and amyloidosis. The beta-fibrilloses (first of two parts). *N. Engl. J. Med.* **302**, 1283–1292 (1980).
- Giasson, B. I., Lee, V. M. & Trojanowski, J. Q. Interactions of amyloidogenic proteins. *Neuromol. Med.* **4**, 49–58 (2003).
- Ly, P. T., Cai, F. & Song, W. Detection of neuritic plaques in Alzheimer's disease mouse model. *J Vis Exp*, e2831–2834 (2011).

6. Darvesh, S. & Reid, G. A. Reduced fibrillar beta-amyloid in subcortical structures in a butyrylcholinesterase-knockout Alzheimer disease mouse model. *Chem. Biol. Interact.* **259**, 307–312 (2016).
7. Fernandez, T., Martinez-Serrano, A., Cusso, L., Desco, M. & Ramos-Gomez, M. Functionalization and characterization of magnetic nanoparticles for the detection of ferritin accumulation in Alzheimer's disease. *ACS Chem. Neurosci.* **9**, 912–924 (2018).
8. Oakley, H. *et al.* Intraneuronal beta-amyloid aggregates, neurodegeneration, and neuron loss in transgenic mice with five familial Alzheimer's disease mutations: potential factors in amyloid plaque formation. *J. Neurosci.* **26**, 10129–10140 (2006).
9. Okamoto, M. *et al.* Riluzole reduces amyloid beta pathology, improves memory, and restores gene expression changes in a transgenic mouse model of early-onset Alzheimer's disease. *Transl. Psychiatry* **8**, 153–165 (2018).
10. Saksida, T. *et al.* Impaired IL-17 production in gut-residing immune cells of 5xFAD mice with Alzheimer's disease pathology. *J. Alzheimers Dis.* **61**, 619–630 (2018).
11. Svensson, M., Andersson, E., Manouchehrian, O., Yang, Y. Y. & Deierborg, T. Voluntary running does not reduce neuroinflammation or improve non-cognitive behavior in the 5xFAD mouse model of Alzheimer's disease. *Sci. Rep.* **10**, 1346–1355 (2020).
12. Kim, H. Y. *et al.* EPPS rescues hippocampus-dependent cognitive deficits in APP/PS1 mice by disaggregation of amyloid-beta oligomers and plaques. *Nat. Commun.* **6**, 8997–9010 (2015).
13. Lalowski, M. *et al.* The “nonamyloidogenic” p3 fragment (amyloid beta 17–42) is a major constituent of Down's syndrome cerebellar preamyloid. *J. Biol. Chem.* **271**, 33623–33631 (1996).
14. Rostagno, A. & Ghiso, J. Isolation and biochemical characterization of amyloid plaques and paired helical filaments. *Curr. Protoc. Cell Biol.* **Chapter 3**, 1–33 (2009).
15. Kim, H. Y., Kim, H. V., Lee, D. K., Yang, S. H. & Kim, Y. Rapid and sustained cognitive recovery in APP/PS1 transgenic mice by co-administration of EPPS and donepezil. *Sci. Rep.* **6**, 34165 (2016).
16. Biernat, J. *et al.* The switch of tau protein to an Alzheimer-like state includes the phosphorylation of two serine-proline motifs upstream of the microtubule binding region. *EMBO J.* **11**, 1593–1597 (1992).
17. Mattsson-Carlsson, N. *et al.* Abeta deposition is associated with increases in soluble and phosphorylated tau that precede a positive Tau PET in Alzheimer's disease. *Sci. Adv.* **6**, eaaz2387 (2020).
18. Cho, H. J., Sharma, A. K., Zhang, Y., Gross, M. L. & Mirica, L. M. A multifunctional chemical agent as an attenuator of amyloid burden and neuroinflammation in Alzheimer's disease. *ACS Chem. Neurosci.* **11**, 1471–1481 (2020).
19. Shukla, V. *et al.* A truncated peptide from p35, a Cdk5 activator, prevents Alzheimer's disease phenotypes in model mice. *FASEB J.* **27**, 174–186 (2013).
20. Augustinack, J. C., Schneider, A., Mandelkow, E. M. & Hyman, B. T. Specific tau phosphorylation sites correlate with severity of neuronal cytopathology in Alzheimer's disease. *Acta Neuropathol.* **103**, 26–35 (2002).
21. Blurton-Jones, M. & Laferla, F. M. Pathways by which Abeta facilitates tau pathology. *Curr. Alzheimer. Res.* **3**, 437–448 (2006).
22. Krivinko, J. M., Koppel, J., Savonenko, A. & Sweet, R. A. Animal models of psychosis in Alzheimer disease. *Am. J. Geriatr. Psychiatry* **28**, 1–19 (2020).
23. Moechars, D. *et al.* Early phenotypic changes in transgenic mice that overexpress different mutants of amyloid precursor protein in brain. *J. Biol. Chem.* **274**, 6483–6492 (1999).
24. Stancu, I. C., Vasconcelos, B., Terwel, D. & Dewachter, I. Models of beta-amyloid induced Tau-pathology: the long and “folded” road to understand the mechanism. *Mol. Neurodegener* **9**, 51–64 (2014).
25. Sturchler-Pierrat, C. *et al.* Two amyloid precursor protein transgenic mouse models with Alzheimer disease-like pathology. *PNAS* **94**, 13287–13292 (1997).

Acknowledgements

This work was supported by Korea Health Industry Development Institute (KHIDI, HI18C0836), National Research Foundation of Korea (NRF-2018R1A6A1A03023718 and NRF-2018M3C7A1021858), and POSCO TJ Foundation (POSCO Science Fellowship).

Author contributions

J.S. and Y.K. designed all experiments and analyses. J.S. and S.P. conducted histochemical analyses. H.L. performed drug administration. J.S., S.P., H.L., and Y.K. wrote the manuscript.

Competing interests

The authors declare no competing interests.

Additional information

Supplementary Information The online version contains supplementary material available at <https://doi.org/10.1038/s41598-021-81304-6>.

Correspondence and requests for materials should be addressed to Y.K.

Reprints and permissions information is available at www.nature.com/reprints.

Publisher's note Springer Nature remains neutral with regard to jurisdictional claims in published maps and institutional affiliations.



Open Access This article is licensed under a Creative Commons Attribution 4.0 International License, which permits use, sharing, adaptation, distribution and reproduction in any medium or format, as long as you give appropriate credit to the original author(s) and the source, provide a link to the Creative Commons licence, and indicate if changes were made. The images or other third party material in this article are included in the article's Creative Commons licence, unless indicated otherwise in a credit line to the material. If material is not included in the article's Creative Commons licence and your intended use is not permitted by statutory regulation or exceeds the permitted use, you will need to obtain permission directly from the copyright holder. To view a copy of this licence, visit <http://creativecommons.org/licenses/by/4.0/>.

© The Author(s) 2021